

# Strong coupling constant from moments of quarkonium correlators revisited

Peter Petreczky · Johannes Heinrich Weber

Received: date / Accepted: date

**Abstract** We revisit previous determination of the strong coupling constant from moments of quarkonium correlators in (2+1)-flavor QCD. We use previously calculated moments obtained with Highly Improved Staggered Quark (HISQ) action for five different quark masses and several lattice spacings. We perform a careful continuum extrapolations of the moments and from the comparison of these to the perturbative result we determine the QCD Lambda parameter,  $\Lambda_{\overline{MS}}^{n_f=3} = 332 \pm 17 \pm 2(\text{scale})$  MeV. This corresponds to  $\alpha_s^{n_f=5}(\mu = M_Z) = 0.1177(12)$ .

**Keywords** Quantum Chromodynamics · Lattice QCD

**PACS** 12.38. Gc, 12.38.-t, 12.38.Bx

---

P. Petreczky

Physics Department, Brookhaven National Laboratory, Upton, NY 11973, USA

E-mail: petreczk@bnl.gov

J. H. Weber

Institut für Physik, Humboldt-Universität zu Berlin & IRIS Adlershof, D-12489 Berlin, Germany

E-mail: johannes.weber@physik.hu-berlin.de

## 1 Introduction

There are many lattice QCD calculations aiming to obtain the strong coupling constant,  $\alpha_s$ , using different methods, since it is important for the precision tests of the Standard Model, see Refs. [1,2] for recent reviews. One of the methods to determine  $\alpha_s$  on the lattice is to consider moments of quarkonium correlators. The method was pioneered by HPQCD collaboration [3] in 2008 and used in many lattice calculations since [4,5,6,7,8]. One of the challenges in this method is to obtain reliable continuum results for the moments of quarkonium correlators. To deal with this problem Bayesian fits have been used in Refs. [3,4,5]. On the other hand the analysis of Refs. [6,8] uses many lattice spacings, utilizing a large set of gauge ensembles from HotQCD collaboration [9,10] as well as additional gauge configurations on very fine lattices with  $a < 0.04$  fm [11]. However, even with eleven different lattice spacings the continuum extrapolation of the moments of quarkonium correlators turned out to be challenging. The continuum extrapolations in Refs. [8] were reasonably stable for  $m_h = m_c$  and  $m_h = 1.5m_c$ . However, for larger heavy-quark masses, namely  $m_h = 2m_c$ ,  $3m_c$  and  $4m_c$  they turned out to be problematic. As the result the strong coupling constant determined from the lattice results for  $m_h = 2m_c$  was significantly lower, and inconsistent with the results obtained at the lowest two quark masses. The  $\alpha_s$  value from the combined analysis at different  $m_h$  therefore turned out to be lower than other determinations from the moments of quarkonium correlators and had large errors. The aim of this paper is to improve the analysis of Ref. [8] at larger quark masses through the combined fits of the lattice results at different quark masses and resolve the above discrepancy. The other problem in the determination of the strong coupling constant is the proper estimate of the perturbative error. This is closely related to the choice of the renormalization scale, which should be proportional to  $m_h$ . In Refs. [3,4,5,7]  $\mu = 3m_h$  was used, while in Refs. [6,8] the renormalization scale  $\mu$  was set

to be equal to  $m_h$ . In this paper we will use many choices of the renormalization scale  $\mu$  and demonstrate the consistency of the corresponding  $\alpha_s$  determinations ensuring that the estimate of the perturbative uncertainties is reliable.

The rest of the paper is organized as follows. In section 2 we review the general aspects of  $\alpha_s$  determination from the moments of quarkonium correlators. In section 3 we discuss the continuum extrapolations of the moments. Section 4 contains the determination of the strong coupling constant. Finally our conclusions are presented in section 5.

## 2 Moments of quarkonium correlators and the strong coupling constant

In this paper we consider moments of the pseudo-scalar quarkonium correlator to determine the strong coupling constant along the lines presented in Ref. [8]. We will discuss the main points of this procedure for completeness. The pseudo-scalar quarkonium correlator is defined as

$$G_n = \sum_t t^n G(t), \quad G(t) = a^6 \sum_{\mathbf{x}} (am_{h0})^2 \langle j_5(\mathbf{x}, t) j_5(0, 0) \rangle. \quad (1)$$

Here  $j_5 = \bar{\psi} \gamma_5 \psi$  is the pseudo-scalar current and  $m_{h0}$  is the lattice heavy-quark mass. One can also consider the vector current, however, the lattice calculations of the corresponding correlation function turned out to be less precise [3]. For a lattice with temporal size  $N_t$  the above definition of the moments can be generalized as follows:

$$G_n = \sum_t t^n (G(t) + G(N_t - t)). \quad (2)$$

In the continuum the moments  $G_n$  are finite only for  $n \geq 4$  ( $n$  even), since the correlation function diverges as  $t^{-4}$  for small  $t$ . Furthermore, the moments  $G_n$  do not need renormalization because the explicit factors of the quark mass are included in their definition [3]. The

moments can be calculated in perturbation theory in  $\overline{MS}$  scheme

$$G_n = \frac{g_n(\alpha_s(\mu), \mu/m_h)}{am_h^{n-4}(\mu_m)}. \quad (3)$$

Here  $\mu$  is the  $\overline{MS}$  renormalization scale. The scale,  $\mu_m$  at which the  $\overline{MS}$  heavy-quark mass is defined could be different from  $\mu$  in general [12]. The coefficient  $g_n(\alpha_s(\mu), \mu/m_h)$  is calculated up to 4-loop, i.e. including the term of order  $\alpha_s^3$  [13, 14, 15].

In lattice calculations it is more practical to consider the reduced moments [3]

$$R_n = \begin{cases} G_n/G_n^{(0)} & (n = 4) \\ (G_n/G_n^{(0)})^{1/(n-4)} & (n \geq 6) \end{cases}, \quad (4)$$

where  $G_n^{(0)}$  is the moment calculated from the free correlation function. The lattice artifacts largely cancel out in these reduced moments.

It is straightforward to write down the perturbative expansion for  $R_n$ :

$$R_n = \begin{cases} r_4 & (n = 4) \\ r_n \cdot (m_{h0}/m_h(\mu_m)) & (n \geq 6) \end{cases}, \quad (5)$$

$$r_n = 1 + \sum_{j=1}^3 r_{nj}(\mu/m_h) \left( \frac{\alpha_s(\mu)}{\pi} \right)^j. \quad (6)$$

From the above equations it is clear that  $R_4$  is suitable for the extraction of the strong coupling constant  $\alpha_s(\mu)$  at scale proportional to the heavy-quark mass,  $m_h$ , while the ratios  $R_n/m_{h0}$  with  $n \geq 6$  are suitable for extracting the heavy-quark mass once  $\alpha_s(\mu)$  is determined. One can also use the ratios of the reduced moments, namely  $R_6/R_8$  and  $R_8/R_{10}$  to determine  $\alpha_s$ . We will discuss these ratios in the Appendix.

### 3 Continuum extrapolations of the reduced moments of quarkonium correlators

In our analysis we used previously published lattice QCD results for the reduced moments in (2+1)-flavor QCD obtained for heavy-quark masses  $m_h = m_c, 1.5m_c, 2m_c, 3m_c$  and  $4m_c$ ,

**Table 1** The continuum results for the reduced moments of quarkonium correlators at different heavy-quark masses. The last column shows the  $\alpha_s$  values extracted from  $R_4$  with  $\mu = m_h$ . The first, second, and third errors in  $\alpha_s$  correspond to the lattice error, the perturbative error, and the error due to the gluon condensate, respectively, see text.

$m_h$	$R_4$	$R_6/m_{c0}$	$R_8/m_{c0}$	$R_{10}/m_{c0}$	$\alpha_s(m_h)$
$1.0m_c$	1.2778(20)	1.0200(16)	0.9166(17)	0.8719(21)	0.3798(28)(31)(22)
$1.5m_c$	1.2303(30)	1.0792(20)	0.9860(20)	0.9462(23)	0.3151(43)(14)(4)
$2.0m_c$	1.2051(37)	1.1182(23)	1.0317(23)	0.9944(26)	0.2804(51)(9)(1)
$3.0m_c$	1.1782(44)	1.1729(27)	1.0923(26)	1.0574(31)	0.2434(61)(5)(0)
$4.0m_c$	1.1631(45)	1.2098(31)	1.1321(30)	1.0985(31)	0.2226(62)(4)(0)

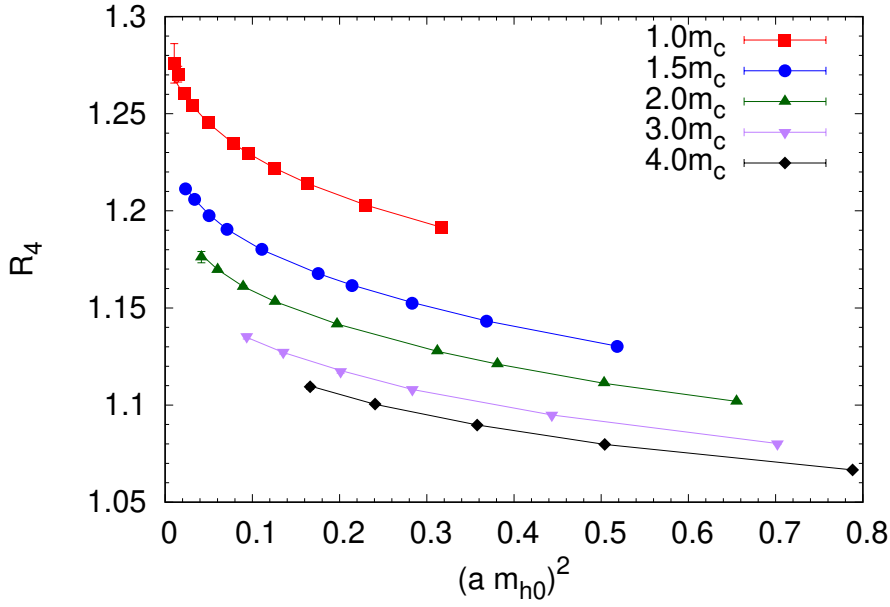


**Fig. 1** The lattice spacing dependence of  $R_4(m_h)$  for different values of the heavy-quark mass. The lines represent the fit with Eq. (8) with  $N = 2$ ,  $M_1 = 8$ ,  $M_2 = 6$  and  $(am_h)_{max}^2 = 0.7$ , see text

with  $m_c$  being the charm-quark mass [8]. The lattice calculations have been performed using HISQ action at several values of the lattice spacing [8]. The lattice spacing has been fixed through the  $r_1$  parameter from the static quark-antiquark potential [9, 10, 11], and the value

$$r_1 = 0.3106(18) \text{ fm} \quad (7)$$

obtained from the pion decay constant was used [16]. Furthermore, the calculations have been performed at two values of the light quark masses corresponding to the pion mass of 161 MeV and 320 MeV in the continuum limit, and no dependence on the light quark mass of the reduced moments was found within errors [8]. The lattice results on  $R_n$ ,  $n = 4, 6, 8, 10$  are found in Tables VII-XI of Ref. [8] for different lattice spacings. The errors in the tables include statistical errors, errors related to mistuning of the charm-quark mass and finite volume errors. All the errors have been added in quadrature. The bare charm-quark masses are found in Table I of [8].

Because the tree-level lattice artifacts cancel out for the reduced moments the lattice spacing dependence can be parameterized as

$$R_4(m_h) = R_4^{cont}(m_h) + \sum_{i=1}^N \sum_{j=1}^{M_i} b_{ij} (\alpha_s^b)^i \left[ 1 + \sum_{k=1}^i d_{ijk} \ln^k(am_{h0}) \right] (am_{h0})^{2j} \quad (8)$$

$$\frac{R_n(m_h)}{m_{h0}} = \left( \frac{R_n(m_h)}{m_{h0}} \right)^{cont} + \sum_{i=1}^N \sum_{j=1}^{M_i} c_{ij}^{(n)} (\alpha_s^b)^i \left[ 1 + \sum_{k=1}^i e_{ijk} \ln^k(am_{h0}) \right] (am_{h0})^{2j}, \quad n \geq 6, \quad (9)$$

where  $\alpha_s^b = g_0^2/(4\pi u_0^4)$ ,  $g_0^2 = 10/\beta$  is the boosted gauge coupling. We performed joint fits of the lattice results on  $R_4$  and  $R_n/m_{h0}$  obtained at different quark masses to Eq. (8) and Eq. (9) setting  $d_{ijk} = e_{ijk} = 0$ . The reason for setting the coefficients of the log terms to zero was to avoid having too many poorly constrained parameters since the logarithmic dependence on  $am_{h0}$  is much weaker than the power-law dependence. For the continuum extrapolations of  $R_4$ , where the lattice spacing dependence is the most prominent, we also performed fits allowing for a few terms proportional to  $\log(am_{h0})$ . These fits are discussed

in the Appendix. Furthermore, the maximal number of terms  $N$  and  $M_i$  in Eqs. (8) and (9) should be sufficiently large so that higher order terms have negligible impact on the continuum extrapolation. The continuum extrapolations of  $R_4$  based on the joint fits of  $m_h = m_c - 4m_c$  lattice data turned out to be much more stable with respect to fit range variations than the extrapolations performed in Ref. [8] separately for each value of  $m_h$ . In particular, there was no problem incorporating  $4m_c$  data in the analysis unlike in Ref. [8], where this was not possible. A sample fit of the data on  $R_4$  is shown in Fig. 1. The joint fits capture the main feature of the data on  $R_4$ , namely the steeper  $a^2$ -dependence for  $R_4(m_c)$  for small lattice spacing and the smaller effective slope of the lattice spacing dependence of the data at larger  $m_h$ , see Fig. 1. The latter observation is the consequence of the fact that many terms contribute to Eq. (8), and often with opposite signs.

To obtain the continuum result for  $R_4$  we performed fits of all available data up to certain maximal value of  $am_{h0}$ , which we denote by  $(am_{h0})_{max}$ . An important consideration in choosing  $(am_h)_{max}$  is the fact that in the free theory the expansion in  $am_{h0}$  converges for  $am_{h0} < \pi/2$  [17]. To be on the safe side we choose  $(am_{h0})_{max}^2 \leq 1.2$  in our analysis. The larger  $(am_{h0})_{max}$  is, the more terms in Eq. (8) should be included. More terms also means more fit parameters, which, however, are difficult to constrain with limited number of data points. We find that using two powers of  $\alpha_s^b$ , i.e.  $N = 2$  is sufficient given our data for  $R_4$ . Fits with  $N > 2$  cannot constrain the parameters. We consider  $(am_{h0})_{max}^2 = 0.4, 0.5, 0.6, 0.7, 0.8, 1.0$  and  $1.2$  and use fits with different  $M_i$ , adjusting it as  $(am_{h0})_{max}$  increases. We do not find significant dependence on  $(am_{h0})_{max}^2$  for the resulting continuum values of  $R_4$ . Furthermore, for a given  $(am_{h0})_{max}$  changing  $M_i$  does not lead to statistically significant differences. For our final continuum values for  $R_4$  we use the results of fits with  $(am_{h0})_{max}^2 = 0.7$ ,  $M_1 = 8$  and  $M_2 = 6$ . The statistical errors of this fit are used as the final error estimates of the continuum result. The continuum results for  $R_4$  for

different quark masses are given in Table 1. For the lowest two quark masses,  $m_h = m_c$  and  $m_h = 1.5m_c$  the continuum results agree well with the ones obtained in Ref. [8], while for the larger quark masses our continuum results are significantly larger.

As a cross-check we also use Akaike information criterion (AIC) [18, 19] to obtain continuum result for  $R_4$  from the performed fits. First, we calculate the AIC weights for each fit and then calculate the weighted average of the fit results with the corresponding weights. Interestingly, this resulted in central values of  $R_4$  very similar to those shown in Table 1. Furthermore, as mentioned above we also performed the continuum extrapolations, which allow for a few terms proportional to  $\log(am_{h0})$ . The corresponding continuum results for  $R_4$  are not significantly different from the ones in Table 1, see Appendix.

To obtain continuum results for  $R_n/m_{h0}$ ,  $n \geq 6$  it is sufficient to consider fits with  $N = 1$  and  $M_1 = 2$ . This is because the errors on  $R_n/m_{h0}$  are much larger than for  $R_4$ . These errors are dominated by the uncertainties in  $m_{h0}$ , which are essentially the uncertainties in  $m_{c0}$  multiplied by the corresponding constant (3/2, 2, 3 and 4). The uncertainties in  $m_{c0}$  come from the errors in tuning the charm-quark mass in the lattice calculations due to the errors of the ground state charmonium mass and the error in the lattice spacing [8]. The errors on  $m_{c0}$  are given in the sixth column of Table 1 in Ref. [8]. We used several values of  $(am_{h0})_{max}$  in our fits. The differences in the central values of  $(R_n/m_{h0})^{cont}$  corresponding to the fits with various  $(am_{h0})_{max}$  turned out to be much smaller than the statistical errors. So one can choose any of these fit results. For the final continuum estimate we choose the fits with the smallest  $\chi^2/df$ , which turned out to be the fits with  $(am_{h0})_{max}^2 = 1.0$  for  $R_6/m_{h0}$  and  $R_8/m_{h0}$ , and the fit with  $(am_{h0})_{max}^2 = 0.8$  for  $R_{10}/m_{h0}$ . The corresponding results are given in Table 1. The new continuum results agree very well with the previous ones but have smaller errors. For some cases the error reduction is significant.



---

#### 4 Determination of the strong coupling constant

Having determined the continuum limit of the reduced moments of quarkonium correlators we are in the position to obtain the strong coupling constant. As discussed in section II the value of  $\alpha_s(\mu)$  can be obtained by comparing  $R_4$  calculated in perturbation theory to the continuum extrapolated lattice result. The renormalization scale  $\mu$  has to be of the order of the heavy-quark mass. We also need to fix the renormalization scale  $\mu_m$  at which the heavy-quark mass is defined. The most natural choice is  $\mu_m = \mu$  and will be used throughout in this paper. We consider the following choices of the renormalization scale,  $\mu/m_h = 2/3, 1, 3/2, 2, 3$ . With these choices of the renormalization scale we can obtain several determinations of  $\alpha_s(\mu)$  which correspond to the lattice results at different values of  $m_h$ , providing important consistency checks, since the composition of the error budget changes with  $m_h$ . There are three sources of errors in  $\alpha_s(\mu)$  determined from  $R_4$ . One that comes from the error on the continuum value of  $R_4$  given in Table 1. There is a perturbative error due to missing higher order corrections. We estimated this error in the same way as in Ref. [8], namely we added a term proportional to  $r_{43}(\alpha_s/\pi)^4$  with the coefficient which was varied between  $-5$  and  $+5$ , to be conservative. Finally, there is an error due to the gluon condensate contribution which was estimated in Ref. [8] by varying the poorly known gluon condensate by factor two.

For larger heavy-quark mass the perturbative error is smaller because the corresponding  $\alpha_s(\mu)$  is smaller. The lattice error on the other hand is larger for larger  $m_h$  since  $R_4$  is closer to one and the relative error on  $R_4$  increases. The error due to the gluon condensate rapidly decreases with increasing  $m_h$  and is negligible for  $m_h > 2m_c$ . As an example we show the values of  $\alpha_s$  for  $\mu = m_h$  in Table 1, which clearly demonstrate these features. The  $\alpha_s(\mu)$  values from the analysis for different choices of  $\mu$  are shown in Fig. 2. In this figure the

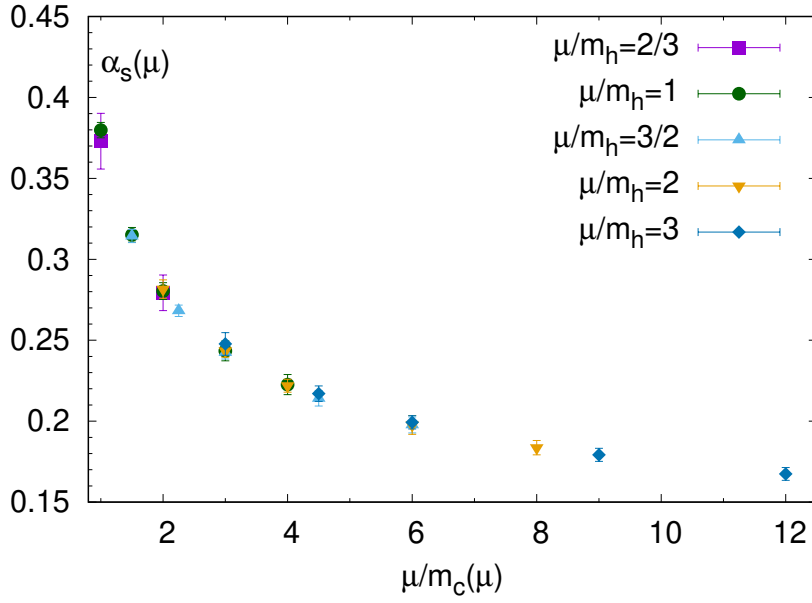


**Fig. 2** The strong coupling constant at different scales proportional to  $m_h$ . The different symbols correspond to the determinations at different values of  $\mu/m_h$ .

different sources of errors have been combined in quadrature. The different symbols in the figure correspond to  $\alpha_s(\mu)$  obtained from  $R_4$  for different choices of  $\mu/m_h$  and agree well within the estimated errors. This is an important consistency check for our procedure and serves as an indication that the errors have been properly estimated.

The above analysis gives values of  $\alpha_s$  at multiple scales proportional to  $m_h(\mu = nm_h)$ ,  $n = 2/3, 1, 3/2, 2, 3$ . But the value of  $m_h(\mu = nm_h)$  was left undetermined. Using the above values of  $\alpha_s(nm_h)$  and the continuum extrapolated lattice results on  $R_n/m_{h0}$  we can easily determine the running charm-quark mass  $m_c(\mu = nm_h) = m_h(\mu = nm_h)/n$ . There are several uncertainties in this determination. One is due to the error in the continuum extrapolated value of  $R_n/m_{h0}$ . The second source of the uncertainty is due to the missing higher order perturbative corrections in  $R_n$ . There is also an uncertainty due to the gluon

condensate contribution. These have been estimated in the same manner as in the case of  $R_4$ . Finally there is an uncertainty due to the error in  $\alpha_s$ . The latter in turn is also affected by the error due to the gluon condensate contribution, which is correlated with the gluon condensate error in  $R_6$ . This correlation should be taken into account. The perturbative error in  $R_4$  and  $R_n$ ,  $n \geq 6$  can be assumed to be uncorrelated. The statistical errors in  $R_4$  and  $R_n$ ,  $n \geq 6$  are of course correlated. However, these errors are sub-dominant. The systematic effects due to the finite volume and mis-tuning of the charm-quark mass are quite different in  $R_4$  and  $R_n$ ,  $n \geq 6$ . Therefore the errors on the continuum values of  $R_4$  and  $R_6/m_{h0}$  are treated as independent. Combining the errors along these lines we show the results on the running charm-quark mass in Fig. 3. The charm-quark mass values determined from  $R_6/m_{c0}$  and  $R_8/m_{c0}$  are shown as filled and open symbols in the figure, and agree well within errors. The charm-quark masses obtained from  $R_{10}/m_{c0}$  are not shown since they appear to be very close to the ones obtained from  $R_8/m_{c0}$ . The values of  $m_c$  determined for different  $\mu/m_h$  but same value of  $\mu$  in GeV also agree with each other except for  $\mu/m_h = 3$ , which are about two sigma lower than the ones for  $\mu/m_h = 1$ , for  $\mu < 5$  GeV. This fact may indicate that the above procedure of estimating the perturbative error due to missing higher order terms was not sufficiently conservative for  $\mu < 5$  GeV. Since the dependence of  $\alpha_s$  on the charm-quark mass is logarithmic the above small inconsistency in  $m_c$  determination is insignificant compared to other sources of errors. We also note that because of the uncertainty in the absolute scale we could not improve significantly the charm-quark mass determination compared to the result of Ref. [8] despite the reduced errors in the continuum values for  $R_n/m_{c0}$ ,  $n \geq 6$ .

Having determined the charm-quark mass we are in a position to obtain the running coupling constant and the  $\Lambda$ -parameter for three-flavor QCD. Using the values of  $\alpha_s$  shown in Fig. 2 and the charm-quark mass at various scales we determine  $\Lambda_{\overline{MS}}^{n_f=3}$  using the RunDec package [20, 21]. We utilize the 5-loop beta function in this study. We use the explicit scheme

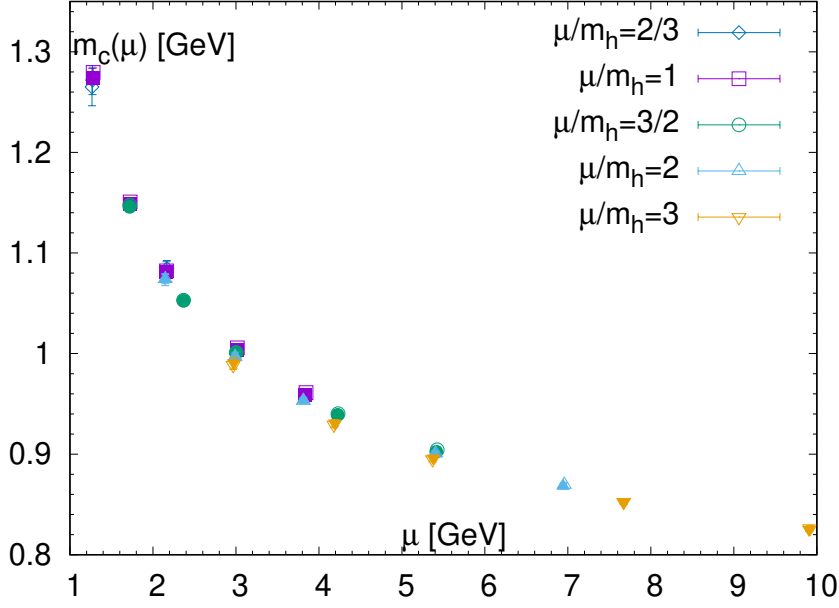


**Fig. 3** The running charm-quark mass. The filled symbols correspond to the determination from  $R_6$ , while the open symbols correspond to the determination from  $R_8$ . The different symbols refer to different choices of  $\mu$  for a given value of  $m_h$ .

**Table 2** The  $\Lambda_{\overline{MS}}^{n_f=3}$  obtained for different values of  $m_h$  and different choices of the renormalization scale. The first error comes from the lattice calculations, the second error is the perturbative error, and the last error is due to the gluon condensate.

$m_h/m_c$	$\mu/m_h = 2/3$	$\mu/m_h = 1$	$\mu/m_h = 3/2$	$\mu/m_h = 2$	$\mu/m_h = 3$
1.0		323(4)(6)(3)	323(4)(7)(3)	327(4)(13)(3)	340(4)(21)(3)
1.5	314(8)(23)(1)	326(9)(4)(1)	326(8)(5)(1)	329(8)(10)(1)	341(9)(18)(1)
2.0		327(13)(3)(0)	327(13)(4)(0)	330(13)(9)(0)	341(14)(16)(0)
3.0	325(20)(20)(0)	332(21)(2)(0)	332(21)(4)(0)	335(22)(22)(0)	344(22)(14)(0)
4.0		336(26)(2)(0)	336(26)(3)(0)	339(27)(7)(0)	347(28)(17)(0)

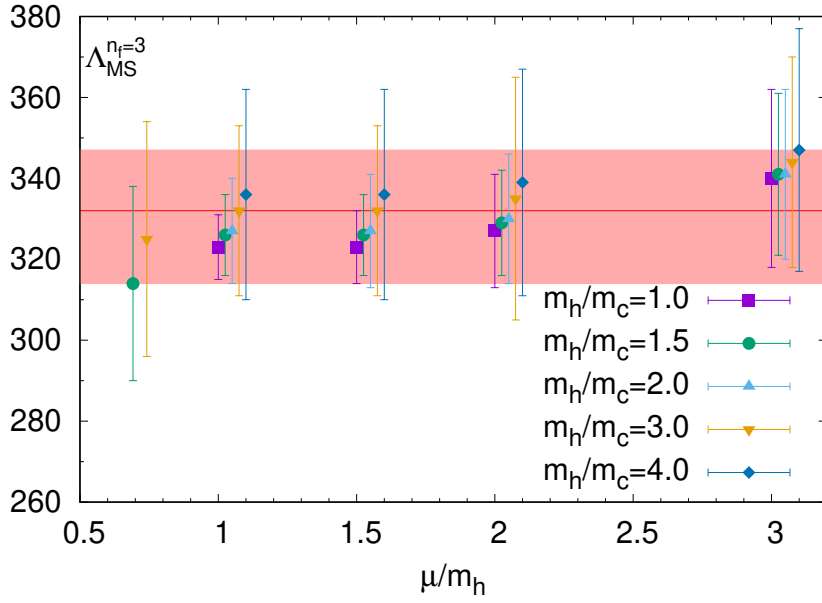


**Fig. 4** The three-flavor Lambda parameter determined for different  $\mu/m_h$ . The different symbols correspond to different values of  $m_h$  and have been slightly shifted horizontally for better visibility. The horizontal line corresponds to the final estimate of  $\Lambda_{MS}^{n_f=3}$  and the band indicates its uncertainty.

defined by Eq. (4) of Ref. [20] to obtain  $\Lambda_{MS}^{n_f=3}$ . We also use the implicit scheme defined by Eq. (5) of Ref. [20] and the difference between the results obtained in explicit and implicit schemes is considered as one of the errors in the determination of the  $\Lambda$  parameter. The other sources of errors include the perturbative errors in the determination of  $m_c$  and  $\alpha_s$  for various  $\mu$ , the lattice errors in these quantities as well as the errors due to the gluon condensate. Our results for  $\Lambda_{MS}^{n_f=3}$  are shown in Table 2. In this Table we show the error budget for the  $\Lambda$ -parameter, including the lattice error, the perturbative error, and the error due to the gluon condensate. The lattice error and the condensate error are obtained by propagating the corresponding errors in  $\alpha_s$  and  $m_c$  taking into account the correlations. The perturbative error shown in Table 2 is obtained by propagating the perturbative error on  $\alpha_s$

and  $m_c$  taking into account the correlations, and adding the error due to scheme dependence (explicit or implicit) in quadrature. From the table we see that the perturbative error in  $\Lambda_{\overline{MS}}^{n_f=3}$  decreases with increasing  $m_h$ , following the trend observed in  $\alpha_s$ , while the lattice error increases. Thus the determination of the  $\Lambda$ -parameter for different heavy-quark masses is complementary and provides an important consistency check. Furthermore, the perturbative error is the smallest for  $\mu = m_h$  and increases when  $\mu \neq m_h$ . In Fig. 4 we show the three-flavor  $\Lambda$ -parameter as function of  $\mu/m_h$ . The different symbols in the figure correspond to different values of  $m_h$  and the errors given in Table 2 were added in quadrature. Looking at the figure one sees that the values of the  $\Lambda$ -parameter obtained for different quark masses and different  $\mu/m_h$  agree well within the estimated errors. On the other hand the values of  $\Lambda_{\overline{MS}}^{n_f=3}$  tend to be larger for larger values of  $\mu/m_h$ . In fact, for the choice  $\mu = 3m_h$  the central value of the  $\Lambda$  parameter is very close to the HPQCD result [4]. Since the errors on  $\Lambda_{\overline{MS}}^{n_f=3}$  determination vary significantly with  $\mu$  and  $m_h$  it is not straightforward to quote a final number for the  $\Lambda$ -parameter. Given the above observations it makes sense to choose a central value for  $\Lambda_{\overline{MS}}^{n_f=3}$  that corresponds to  $m_h$  and  $\mu$  in the middle of the range used in this study. The continuum extrapolation for  $R_4$  for  $m_h = m_c$  and  $m_h = 1.5m_c$  is quite robust since the results presented in this study and in Ref. [8], which uses a different strategy, agree with each other. The perturbative error for  $\mu = 2m_h$  is also not too large. Therefore, the value of  $\Lambda_{\overline{MS}}^{n_f=3} = 329(14)$  MeV obtained for  $m_h = 1.5m_c$  and  $\mu = 2m_h$  can be considered as a representative one. Alternatively we can average over different values to obtain the final estimate of the  $\Lambda$ -parameter. Since the errors of different  $\Lambda_{\overline{MS}}^{n_f=3}$  determinations are correlated we use an unweighted average. This gives  $\Lambda_{\overline{MS}}^{n_f=3} = 331.8$  MeV. Therefore, we take 332 MeV for the central value of the three-flavor  $\Lambda$  parameter. We also consider the weighted average of the result in Fig. 4 using the perturbative error and the error due to scheme choice added in quadrature, since these errors can be assumed to be uncorrelated for different  $m_h$  and  $\mu$ .

This results in  $\Lambda_{\overline{MS}}^{n_f=3} = 331.4$  MeV, which is very close to the above value. We assign an error to  $\Lambda_{\overline{MS}}^{n_f=3}$  such that all central values in Fig. 4 are covered by it. This results in 17 MeV as our error estimate for the  $\Lambda$  parameter, Thus, taking into account the uncertainty in the absolute scale (from  $r_1$ ) our final result reads:

$$\Lambda_{\overline{MS}}^{n_f=3} = 332 \pm 17 \pm 2 \text{ (scale) MeV.} \quad (10)$$

Our error estimate for the  $\Lambda_{\overline{MS}}^{n_f=3}$  parameter is quite conservative and is significantly larger than the one by HPQCD collaboration [4]. This is due to the absence of Bayesian priors and different choices of the renormalization scale  $\mu$  and not just  $\mu = 3m_h$ . We compare our results for the  $\Lambda$ -parameter with other three-flavor lattice determinations, namely from the moments of quarkonium correlators [4], from the static quark anti-quark potential [22, 23, 24], from step-scaling analysis by ALPHA collaboration [25], from ghost-gluon vertex in Landau gauge [26], and from the light quark vector current correlator [27]. This comparison is shown Fig. 5. We see that our result is consistent with other lattice determinations.

For phenomenological applications it is important to know the strong coupling constant in the five-flavor theory at the scale of the Z-boson mass,  $M_Z$ . This can be obtained from the above result for  $\Lambda_{\overline{MS}}^{n_f=3}$  by using the perturbative running of the coupling constant and decoupling at the charm and bottom thresholds. We use the RunDeC package [20, 21] to do this with the 5-loop beta function. There are several ways we can proceed using the RunDeC package. From the  $\Lambda$  parameter in Eq. (10) we can determine  $\alpha_s$  at the decoupling scale  $\mu_c$ , where we match it to the four-flavor coupling using the  $\overline{MS}$  charm-quark mass  $m_c(\mu_c)$  with the help of *DecAsUpMS* routine [20, 21]. A reasonable choice of scale  $\mu_c$  should be between  $m_c(m_c)$  and 2 GeV. Then we evolve the four-flavor coupling to scale  $\mu_b$  where we perform the matching to the five-flavor theory using  $\overline{MS}$  bottom quark mass  $m_b(\mu_b)$  (using *DecAsUpMS* routine), and finally we evolve  $\alpha_s^{n_f=5}(\mu_b)$  to  $\mu = M_Z$ . The scale  $\mu_b$  should be around the

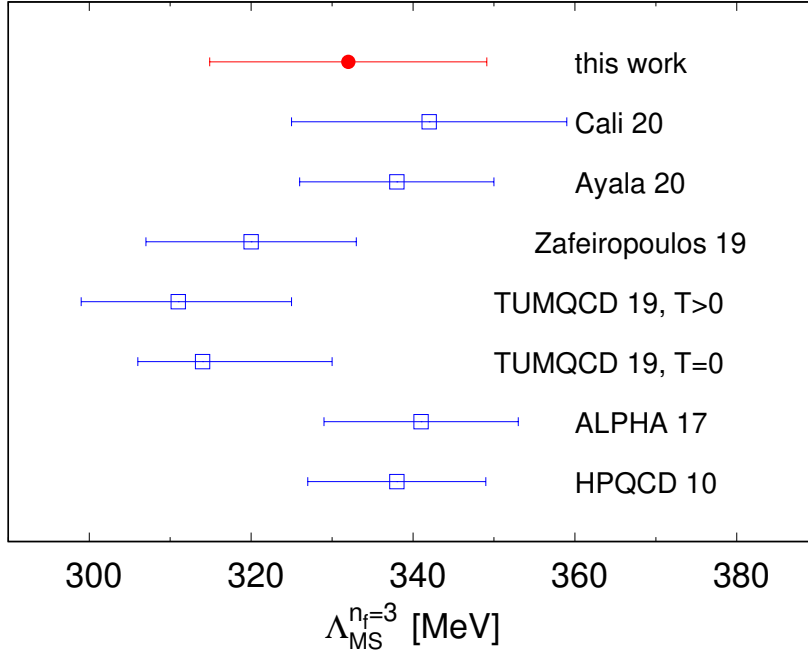


**Fig. 5** Comparison of the  $\Lambda$ -parameter in three-flavor QCD from Refs. [4, 25, 23, 24, 26, 27] (from left to right) to the present determination. The result of Ref. [22] are not shown as these are superseded by Ref. [23].

bottom quark mass. The running charm-quark mass in  $\overline{MS}$  scheme is obtained from  $R_8$  as described above. In this study we use  $\mu_b = m_b(m_b) = 4.188(10)$  obtained from averaging the available lattice results [2] and  $\mu_c = m_c(\mu_c)$ ,  $\mu_c = 1.5m_c(\mu_c)$  and  $\mu_c = 2m_c(\mu_c)$ . This results in  $\alpha_s^{n_f=5}(\mu = M_Z) = 0.117668$ ,  $0.117727$  and  $0.117757$ , respectively. The uncertainty in  $m_b(m_b)$  leads to much smaller spread in the resulting  $\alpha_s^{n_f=5}(\mu = M_Z)$  then above, and therefore, will be neglected. Similarly the effect of varying the scale  $\mu_b$  also leads to smaller variations in  $\alpha_s^{n_f=5}(\mu = M_Z)$ . We can repeat the above procedure using the pole (on-shell) masses  $M_c$  and  $M_b$  of the charm and bottom quark instead of the  $\overline{MS}$  masses and also set  $\mu_c = M_c$  and  $\mu_b = M_b$  with the help of the *DecAsUpOS* routine [20, 21]. This gives  $\alpha_s^{n_f=5}(\mu = M_Z) = 0.118046$  if the RunDeC default values  $M_c = 1.5$  GeV and  $M_b = 4.8$  GeV



are used. Finally, we can match the three-flavor  $\Lambda$  parameter to the four-flavor one, and then the four-flavor  $\Lambda$  parameter to  $\Lambda_{\overline{MS}}^{n_f=5}$  with the help of *DecLambdaUp* routine [20,21] and the values of  $m_c(m_c)$  and  $m_b(m_b)$  above. From this we obtain  $\alpha_s^{n_f=5}(\mu = M_Z) = 0.117952$ . Using the above considerations we choose 0.117727 as our central value value for  $\alpha_s^{n_f=5}(\mu = M_Z)$  and assign an uncertainty of 0.00032 for the running and decoupling procedure. Finally, the uncertainty in  $\Lambda_{\overline{MS}}^{n_f=3}$  translates into an error of 0.00115 for  $\alpha_s^{n_f=5}(\mu = M_Z)$ . Combining this with the uncertainty of the running and the matching in quadrature we obtain

$$\alpha_s^{n_f=5}(\mu = M_Z) = 0.1177(12). \quad (11)$$

This value of  $\alpha_s^{n_f=5}$  agrees with other determinations from the moments of quarkonium correlators within errors [3,4,5,7,28]. It also agrees with the averaged  $\alpha_s^{n_f=5}$  from lattice determinations [1,2].

Before closing this section let us discuss the determination of the strong coupling constant from the ratios  $R_6/R_8$  and  $R_8/R_{10}$ . As mentioned in section II the heavy-quark mass drops out in these ratios and therefore they are well suited for the determination of  $\alpha_s$ . Naively, one would expect that the continuum extrapolation of these ratios is simpler than for  $R_4$  as the higher order moments are less sensitive to the short distance physics. Using such reasonings in Ref. [7] the strong coupling constant was determined using only these ratios. The ratios  $R_6/R_8$  and  $R_8/R_{10}$  have been also used in an attempt to determine  $\alpha_s$  with additional cross-checks [8]. It turns out, however, that the cutoff dependence of  $R_6/R_8$  and  $R_8/R_{10}$  is far from simple, and it is challenging to describe it quantitatively. Furthermore, the finite volume effects are also significant for these ratios. The continuum extrapolations for  $R_6/R_8$  and  $R_8/R_{10}$  from simultaneous fits of the lattice data at different quark masses are discussed in the Appendix. We explain there why these continuum extrapolations are difficult. It turns out that in order to obtain consistent  $\alpha_s$  determination from these ratios additional

priors have to be imposed. The continuum results for  $R_6/R_8$  at  $m_h = m_c$  and  $m_h = 1.5m_c$  are consistent with the previous results [8]. However, it is not possible to obtain reliable continuum results for  $R_6/R_8$  for  $m_h > 2m_c$ . In the case of  $R_8/R_{10}$  the finite volume effects are quite severe for  $m_h = m_c$  and therefore, reliable continuum results can be obtained only for  $m_h \geq 1.5m_c$ . The continuum results for  $R_8/R_{10}$  turned out to be systematically larger than in Ref. [8]. As the result the corresponding  $\alpha_s$  values are larger than the  $\alpha_s$  values obtained from  $R_8/R_{10}$  in Ref. [8] and agree well with the corresponding ones obtained from  $R_4$ . On the other side the strong coupling constant extracted from  $R_8/R_{10}$  has larger error and therefore, does not improve the precision of our  $\alpha_s$  determination. Nevertheless, it does provide a useful cross-check of our analysis.

## 5 Conclusion

In this paper we revisited the determination of the strong coupling constant from the moments of quarkonium correlators. Using previously published lattice results on the reduced moments in (2+1)-flavor QCD with heavy-quark masses  $m_h = m_c, 1.5m_c, 2m_c, 3m_c$  and  $4m_c$  at several lattice spacings we estimated the continuum results on the fourth moment. These estimates were based on simultaneous fits of the lattice spacing dependence of the reduced moments at several quark masses, similar to the analysis of HPQCD collaboration [4,5]. The new continuum estimates turned out to be much more robust compared to the ones obtained from fits of the cutoff dependence of  $R_4$  performed separately for each quark mass [8]. While both studies use the same form to parameterize the cutoff dependence of  $R_4$ , there is an essential difference. The present analysis strongly relies on the specific form of the cutoff dependence given by Eqs. (8) and (12), while in Ref. [8] it is just an effective way to parameterize the lattice spacing dependence of these quantities, and is not essential

for the final continuum result. In this study we constrain the lattice spacing dependence at each heavy-quark mass with the lattice spacing dependence of all other heavy-quark masses, while the previous analysis in Ref. [8] permitted independent variation of the coefficients at different heavy-quark masses. The continuum results at  $m_c$  and  $1.5m_c$  are in good agreement in these approaches. This is reassuring for controlling the continuum extrapolation of these quantities at least for the two lower values of the quark masses. We also revisited the continuum extrapolations of  $R_6/R_8$  and  $R_8/R_{10}$  using simultaneous fits of the lattice results at different quark masses. We have shown that the apparent weaker cutoff dependence of these ratios is misleading, and reliable continuum extrapolations are challenging. We were able to obtain reliable continuum extrapolations for  $R_6/R_8$  only for  $m_h \leq 2m_c$ . For  $R_8/R_{10}$  reliable continuum results are available only for  $m_h > m_c$  because of the finite volume effects.

Comparing the continuum extrapolated results for  $R_4$  for  $m_h = m_c - 4m_c$  and several values of the renormalization scale  $\mu$  we determined the  $\Lambda$  parameter in three-flavor QCD and the running of the strong coupling constant in the range 1.3 GeV to 10 GeV, which is not accessible experimentally. The use of different renormalization scales provides an important consistency check of the estimated perturbative errors. Additional consistency check for  $\alpha_s$  determination comes from the calculation of  $R_8/R_{10}$ .

The obtained value of  $\Lambda_{\overline{MS}}^{n_f=3}$  agrees well with other recent lattice determinations. Performing the running of  $\alpha_s$  to larger scales and decoupling at the charm and bottom thresholds we obtain  $\alpha_s^{n_f=5}(\mu = M_Z) = 0.1177(12)$  that is in good agreement with FLAG as well as the PDG average. Finally, it is reassuring to see that previous inconsistencies in the determination of  $\alpha_s$  from the moments of quarkonium correlators have been resolved.

**Acknowledgements** PP was supported by U.S. Department of Energy under Contract No. DE-SC0012704. JHW's reserch was funded by the Deutsche Forschungsgemeinschaft (DFG, German Research Foundation)

$m_h/m_c$	fit 1	fit 2	fit 3	fit 4	fit 5
1.0	1.2805(14)	1.2782(10)	1.2817(18)	1.2810(13)	1.2806(10)
1.5	1.2308(14)	1.2286(10)	1.2318(16)	1.2309(12)	1.2302(10)
2.0	1.2045(14)	1.2024(09)	1.2053(15)	1.2044(11)	1.2038(10)
3.0	1.1763(15)	1.1743(10)	1.1770(15)	1.1759(11)	1.1754(10)
4.0	1.1608(14)	1.1582(10)	1.1610(15)	1.1601(11)	1.1595(10)

**Table 3** The continuum extrapolated values of  $R_4$  at different heavy quark masses,  $m_h$  from different fits which include terms proportional to  $\log(am_{h0})$ , see text.

- Projektnummer 417533893/GRK2575 “Rethinking Quantum Field Theory”, and by U.S. Department of Energy, Office of Science, Office of Nuclear Physics and Office of Advanced Scientific Computing Research within the framework of Scientific Discovery through Advance Computing (SciDAC) award Computing the Properties of Matter with Leadership Computing Resources.

## A Continuum extrapolation of the ratios and $\alpha_s$ determination

In this appendix we discuss continuum extrapolations for  $R_4$  which allow for terms proportional to  $\log(am_{h0})$ . Furthermore, we discuss the continuum extrapolations of the ratios  $R_6/R_8$  and  $R_8/R_{10}$  and the determination of  $\alpha_s$  from these ratios.

As discussed in the main text including terms proportional to  $\log(am_{h0})$  is challenging as the logarithmic dependence on  $am_{h0}$  is much weaker than the power-law dependence. Therefore, only a few logarithmic terms can be included in the fits to avoid over-fitting and the number of terms in Eq. (8) should be also reduced. We performed five different fits using different values of  $(am_{h0})_{max}^2$  and non-zero values of  $d_{111}$  and  $d_{121}$  and all other  $d_{ijk}$  set to zero. We performed the following fits:

- fit 1:  $(am_{h0})_{max}^2 = 0.4$ ,  $M_1 = 3$ ,  $M_2 = 2$ ,  $d_{111} \neq 0$
- fit 2:  $(am_{h0})_{max}^2 = 0.6$ ,  $M_1 = 3$ ,  $M_2 = 2$ ,  $d_{111} \neq 0$
- fit 3:  $(am_{h0})_{max}^2 = 0.8$ ,  $M_1 = 4$ ,  $M_2 = 2$ ,  $d_{111} \neq 0$
- fit 4:  $(am_{h0})_{max}^2 = 1.0$ ,  $M_1 = 3$ ,  $M_2 = 2$ ,  $d_{111} \neq 0$ ,  $d_{121} \neq 0$
- fit 5:  $(am_{h0})_{max}^2 = 1.2$ ,  $M_1 = 4$ ,  $M_2 = 2$ ,  $d_{111} \neq 0$ ,  $d_{121} \neq 0$

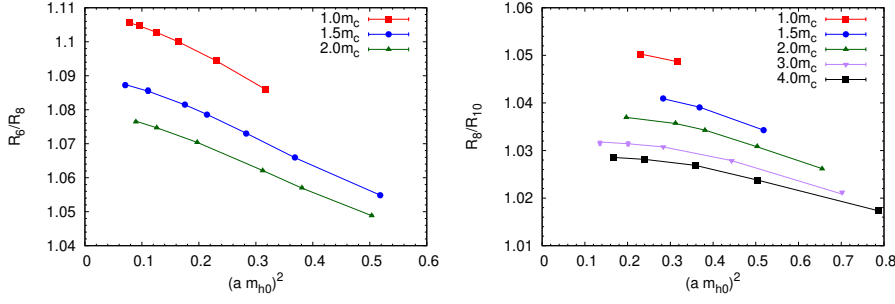


**Fig. 6** The lattice results and the continuum extrapolations (fits) for  $R_6/R_8$  (left) and  $R_8/R_{10}$  (right), see text

These were the only possible fits that avoided over-fitting. The continuum extrapolated values of  $R_4$  from fit 1-5 are given in 3. As one can see from the table the continuum  $R_4$  values agree with the ones presented in the main text within errors but have smaller errors. Thus the inclusions of terms proportional to  $\log(am_{h0})$  does not lead to significant changes in the continuum extrapolated value of  $R_4$ . Since we want to have conservative error estimates for the continuum results on  $R_4$  we use the values presented in the main text.

As discussed in the main text it is also possible to determine the strong coupling constant from the ratios  $R_6/R_8$  and  $R_8/R_{10}$  as the heavy-quark mass drops out in these ratios. The apparent cutoff dependence of the ratios  $R_6/R_8$  and  $R_8/R_{10}$  calculated on the lattice is indeed smaller than for  $R_4$  [8]. As we have seen above, to describe the cutoff dependence of  $R_4$  many powers of  $am_{h0}$  are needed and the coefficients often have opposite signs from one order in  $(am_{h0})^2$  to the next one. Therefore, the apparent cutoff dependence of  $R_4$  turns out to be smaller as we increase the heavy-quark mass contrary to the naive expectations. The situation could be similar for  $R_6/R_8$  and  $R_8/R_{10}$ . Furthermore, the cutoff dependence of the numerator and denominator, while being significant, could cancel out in the ratios, thus fooling one into thinking that cutoff effects are small and can be modeled with a low order polynomial in  $(am_{h0})^2$ . We should keep these issues in mind when performing continuum extrapolations of the ratios.

To obtain the continuum result for  $R_6/R_8$  we perform simultaneous fits of the lattice data at different quark masses to

$$\frac{R_n(m_h)}{R_{n+2}(m_h)} = \left( \frac{R_n(m_h)}{R_{n+2}(m_h)} \right)^{cont} + \sum_{i=1}^N \sum_{j=1}^{M_i} f_{ij}^{(n)} (\alpha_s^b)^i (am_{h0})^{2j}, \quad n \geq 6. \quad (12)$$

As in Ref. [8] we omit data on fine lattices to avoid finite volume effects when performing fits. The  $\chi^2/df$  of the fit is large unless we use high order polynomials in  $(am_{h0})^2$ . However, using high order polynomials in the fit results in many poorly constrained parameters. Furthermore, a closer look at the lattice data reveals that the slope of the  $(am_{h0})^2$  dependence is quite different for various  $m_h$ , explaining why  $\chi^2/df$  is large. The apparent

**Table 4** The continuum values of the ratios  $R_6/R_8$  and  $R_8/R_{10}$  and the corresponding coupling constants  $\alpha_s(\mu = m_h)$  for different values of the heavy-quark masses  $m_h$ , see text.

$R_6/R_8$			$R_8/R_{10}$		
$m_h/m_c$	continuum	$\alpha_s(m_h)$	$m_h/m_c$	continuum	$\alpha_s(m_h)$
1.0	1.10895(32)	0.3826(14)(178)(39)	1.0	-	-
1.5	1.09100(25)	0.3137(10)(76)(8)	1.5	1.04310(45)	0.3166(34)(82)(17)
2.0	-	-	2.0	1.03830(68)	0.2808(51)(50)(4)
3.0	-	-	3.0	1.03249(94)	0.2382(69)(24)(1)
4.0	-	-	4.0	1.02987(106)	0.2191(293)(17)(0)

slope also decreases with increasing  $m_h$ , indicating that consecutive terms in Eq. (12) have opposite signs. To deal with these problems we omit lattice results for  $m_h \geq 3m_c$ . Including these data will require adding many more parameters in Eq. (12) which are difficult to constrain with the relatively few additional data points coming from the  $m_h = 3m_c$  and  $m_h = 4m_c$  data set. We also set the continuum value of  $R_6/R_8$  at  $2m_c$  to the one obtained in perturbation theory with  $\alpha_s(2m_c)$  inferred from the continuum results on  $R_4$  at  $2m_c$ . The continuum values of  $R_6/R_8$  for  $m_h = m_c$  and  $1.5m_c$  are treated as fit parameters. Keeping terms up to  $N = 2$  and  $M_1 = M_2 = 3, 4$  is sufficient to obtain good fits in the interval  $(0, (am_{h0})_{max}^2)$  with  $(am_{h0})_{max}^2 = 0.4 - 0.6$ . The fit for  $(am_{h0})_{max}^2 = 0.6$  as well as the main features of the lattice data for  $R_6/R_8$  are demonstrated in Fig. 6. No significant dependence of the continuum result on  $(am_{h0})_{max}^2$  have been found. We choose results of fits with  $(am_{h0})_{max}^2 = 0.6$  for the final continuum estimate, which are shown in Table 4. We also used AIC to obtain the continuum values and these were very close to the central value from the above fits. The new continuum estimate for  $R_6/R_8$  agree with the results of Ref. [8] within errors.

From the continuum results on  $R_6/R_8$  at  $m_c$  and  $1.5m_c$  we determine the corresponding  $\alpha_s(m_h)$  by comparing to the 4-loop perturbative results, which are also given in Table 4. The different sources of errors are estimated in the same way as for  $R_4$ . The perturbative error turns out to be larger in this case. We see from the table that the  $\alpha_s$  values agree with the ones obtained from  $R_4$  at  $\mu = m_c$  and  $\mu = 1.5m_c$ , c.f. Table 1. While we were not able to obtain continuum result for  $R_6/R_8$  for  $m_h = 2m_c$  we demonstrated that the lattice results on  $R_6/R_8$  are compatible with the  $\alpha_s$  values obtained at smaller quark masses if the cutoff dependence is properly taken into account. Therefore, the previous inconsistencies in the determination of  $\alpha_s$  from the lattice data at  $2m_h$  [8] are now resolved.

Next we perform the continuum extrapolation for  $R_8/R_{10}$ . As for  $R_6/R_8$  we fit the cutoff dependence of the lattice results at different quark masses with Eq. (12). The finite volume effects are the largest for  $R_{10}$  and thus for  $R_8/R_{10}$ , and it is possible that the finite volume errors in Ref. [8] were not adequate for many of the  $\beta$  values, especially in the case of  $m_h = m_c$ . This may explain why the  $\alpha_s$  values obtained from  $R_8/R_{10}$  were systematically lower [8]. For the ratio  $R_8/R_{10}$  at  $m_h = m_c$  perturbation theory would predict a value 1.0516 if  $\alpha_s(m_c)$  obtained from  $R_4$  is used. In the data, the ratio reaches the maximal value of 1.05043 at  $\beta = 7.15$ , and the central values monotonically decrease with increasing  $\beta$ , i.e. when approaching the continuum. Thus, there is a clear tension between the continuum value of  $R_8/R_{10}$  and the analysis of  $R_4$  and  $R_6/R_8$  at  $m_h = m_c$  if the lattice results at large  $\beta$  are taken at a face value independently of the details of the continuum extrapolations. Furthermore, the central values of  $R_8/R_{10}$  also show non-monotonic behavior in  $\beta$  for  $6.74 \leq \beta \leq 7.28$ . We interpret this as indication that the finite volume errors are not under control for  $\beta > 6.88$  and  $m_h = m_c$ . We note that the low central value of  $R_8/R_{10}$  is not unique to Ref. [8] but has been seen in other works [3, 6, 7] as well with the exception of Ref. [4]. The non-monotonic dependence of  $R_8/R_{10}$  with increasing  $\beta$  is also observed for  $m_h = 1.5m_c$  and  $2m_c$  but the maximum is shifted to significantly larger values of  $\beta$ . Finally, for  $m_h = 3m_c$  and  $4m_c$  this non-monotonic behavior cannot be clearly observed because of the large errors on the finest lattices. The above differences in the cutoff dependence of  $R_8/R_{10}$  at different quark masses make a simultaneous fit of the cutoff dependence very difficult. This difficulty is likely related to the finite volume effects. To solve this problem we discard data on  $R_8/R_{10}$  with small spatial extent. For  $m_h = m_c$  the finite volume effects are under control for  $\beta$  up to  $\beta = 6.88$ , which corresponds to the bare charm-quark mass  $am_{c0} = 0.48$  and spatial extent  $N_s = 48$  (c.f. Table I in Ref. [8]). Therefore, we only include data with  $L_s m_{h0} \geq 23$  in the fit. Since for  $m_h = m_c$  there are only two data points satisfying this condition the continuum value of  $R_8(m_c)/R_{10}(m_c)$  was fixed to the perturbative result above (1.0516). With this cut and constraint the joint fits have good  $\chi^2/df$  and the fit results are robust with respect to variation of the upper limit of the fit range,  $(am_{h0})_{max}^2$ , which was varied from 0.5 to 1.1. The number of terms in the fit Ansatz had to be adjusted accordingly. For  $(am_{h0})_{max}^2 = 0.5$  we used  $N = 2$ ,  $M_1 = 3$  and  $M_2 = 2$ , while for  $(am_{h0})_{max}^2 = 1.1$  we used  $N = 2$ ,  $M_1 = 5$  and  $M_2 = 4$ . For the final continuum estimate we use the fit with  $(am_{h0})_{max}^2 = 0.8$ ,  $N = 2$ ,  $M_1 = 4$  and  $M_2 = 3$ . This fit is shown in Fig. 6 together with the lattice data on  $R_8/R_{10}$ . The corresponding continuum results for  $R_8/R_{10}$  are shown in Table 4. We also applied the AIC to different fit results and the resulting continuum estimates turned out to be close to the central value of the fit with  $(am_{h0})_{max}^2 = 0.8$ . From the continuum values for  $R_8/R_{10}$  in Table 4 we determine  $\alpha_s(m_h)$  by comparing

to the perturbative result for  $\mu = m_h$ . These values are in good agreement with the  $\alpha_s(m_h)$  values obtained from  $R_4$  within errors, see Tables 1 and 4. Thus, we have an additional cross-check for  $\alpha_s$  determination at scales  $\mu = 1.5m_c - 4m_c$ .

## References

1. S. Aoki, et al., *Eur. Phys. J. C* **80**(2), 113 (2020). DOI 10.1140/epjc/s10052-019-7354-7
2. J. Komijani, P. Petreczky, J.H. Weber, *Prog. Part. Nucl. Phys.* **113**, 103788 (2020). DOI 10.1016/j.pnpnp.2020.103788
3. I. Allison, et al., *Phys. Rev.* **D78**, 054513 (2008). DOI 10.1103/PhysRevD.78.054513
4. C. McNeile, C.T.H. Davies, E. Follana, K. Hornbostel, G.P. Lepage, *Phys. Rev.* **D82**, 034512 (2010). DOI 10.1103/PhysRevD.82.034512
5. B. Chakraborty, C.T.H. Davies, B. Galloway, P. Knecht, J. Koponen, G. Donald, R. Dowdall, G. Lepage, C. McNeile, *Phys. Rev.* **D91**(5), 054508 (2015). DOI 10.1103/PhysRevD.91.054508
6. Y. Maezawa, P. Petreczky, *Phys. Rev.* **D94**(3), 034507 (2016). DOI 10.1103/PhysRevD.94.034507
7. K. Nakayama, B. Fahy, S. Hashimoto, *Phys. Rev.* **D94**(5), 054507 (2016). DOI 10.1103/PhysRevD.94.054507
8. P. Petreczky, J. Weber, *Phys. Rev. D* **100**(3), 034519 (2019). DOI 10.1103/PhysRevD.100.034519
9. A. Bazavov, et al., *Phys. Rev. D* **85**, 054503 (2012). DOI 10.1103/PhysRevD.85.054503
10. A. Bazavov, et al., *Phys. Rev.* **D90**, 094503 (2014). DOI 10.1103/PhysRevD.90.094503
11. A. Bazavov, P. Petreczky, J.H. Weber, *Phys. Rev.* **D97**(1), 014510 (2018). DOI 10.1103/PhysRevD.97.014510
12. B. Dehnadi, A.H. Hoang, V. Mateu, *JHEP* **08**, 155 (2015). DOI 10.1007/JHEP08(2015)155
13. C. Sturm, *JHEP* **09**, 075 (2008). DOI 10.1088/1126-6708/2008/09/075
14. Y. Kiyo, A. Maier, P. Maierhofer, P. Marquard, *Nucl. Phys.* **B823**, 269 (2009). DOI 10.1016/j.nuclphysb.2009.08.010
15. A. Maier, P. Maierhofer, P. Marquard, A.V. Smirnov, *Nucl. Phys.* **B824**, 1 (2010). DOI 10.1016/j.nuclphysb.2009.08.011
16. A. Bazavov, et al., *PoS LATTICE2010*, 074 (2010)
17. A. Bazavov, et al., *Phys. Rev.* **D98**(7), 074512 (2018). DOI 10.1103/PhysRevD.98.074512
18. H. Akaike, *IEEE Transactions on Automatic Control* **19**, 716 (1974)



- 
19. J.M. Cavanaugh, *Statistics & Probability Letters* **33**, 201 (1997)
  20. K.G. Chetyrkin, J.H. Kuhn, M. Steinhauser, *Comput. Phys. Commun.* **133**, 43 (2000). DOI 10.1016/S0010-4655(00)00155-7
  21. F. Herren, M. Steinhauser, *Comput. Phys. Commun.* **224**, 333 (2018). DOI 10.1016/j.cpc.2017.11.014
  22. A. Bazavov, N. Brambilla, X. Garcia i Tormo, P. Petreczky, J. Soto, A. Vairo, *Phys. Rev.* **D90**(7), 074038 (2014). DOI 10.1103/PhysRevD.90.074038
  23. A. Bazavov, N. Brambilla, X. Garcia i Tormo, P. Petreczky, J. Soto, A. Vairo, J.H. Weber, *Phys. Rev. D* **100**(11), 114511 (2019). DOI 10.1103/PhysRevD.100.114511
  24. C. Ayala, X. Lobregat, A. Pineda, *JHEP* **09**, 016 (2020). DOI 10.1007/JHEP09(2020)016
  25. M. Bruno, M. Dalla Brida, P. Fritzscht, T. Korzec, A. Ramos, S. Schaefer, H. Simma, S. Sint, R. Sommer, *Phys. Rev. Lett.* **119**(10), 102001 (2017). DOI 10.1103/PhysRevLett.119.102001
  26. S. Zafeiropoulos, P. Boucaud, F. De Soto, J. Rodríguez-Quintero, J. Segovia, *Phys. Rev. Lett.* **122**(16), 162002 (2019). DOI 10.1103/PhysRevLett.122.162002
  27. S. Cali, K. Cichy, P. Korcyl, J. Simeth, *Phys. Rev. Lett.* **125**, 242002 (2020). DOI 10.1103/PhysRevLett.125.242002
  28. D. Boito, V. Mateu, *JHEP* **03**, 094 (2020). DOI 10.1007/JHEP03(2020)094